INVESTIGATION OF SINGLE-MODE CHARACTERISTICS AND MODE AREA OF PCF WITH SOLID-CORE FOR FIXED HOLE-DIAMETER AND FIXED PITCH LENGTH

Halime Demir INCI[1]

In this study, the single-mode behavior and the mode-field areas of the photonic crystal fibers with triangular lattice for both the structures with a fixed hole-diameter (d) and with a fixed pitch length (Λ) are investigated comparatively. It is found from the simulations that, in order to conclude the photonic crystal fiber is in the single-mode regime or not, there is no significant difference between using the direct evaluation of the V-parameter of photonic crystal fiber and step-index fiber analogy, and for the fixed hole-diameter, effective V-parameter decreases with wavelength and reaches the single-mode limit more rapidly than those for fixed pitch length structures for especially $d/\Lambda > d^*/\Lambda$.. Effective mode area of photonic crystal fibers considered is larger for the fixed pitch length than those of the fixed hole-diameter structures for every d/Λ ratio and reaches some values larger than 1000 μm^2 for the d/Λ values smaller than 0.2.

Keywords: photonic crystal fibers, single mode, solid-core.

1. Introduction

A new class of fibers, so-called Photonic Crystal Fibers (PCFs) or Microstructured Optical Fibers (MOFs), have attracted a great interest. PCFs have two different guiding mechanism as index guiding (IG) [1] and bandgap guiding (BG) [2]. In the recent study, a new type of PCF which uses both mechanism at the same time to confine the light called as Hybrid PCFs has been proposed. [3]. In IG-PCFs, the light is guided in a higher index core by modified total internal reflection from photonic crystal cladding with low effective index. In BG-PCFs, by trapping the light having wavelength falling in the bandgap of photonic crystal structure in the cladding, light is confined in a low index core region. Due to the novel guiding mechanism and different design, these fibers have significant applications and several novel properties. These novel properties of IG-PCFs involve dispersion management [9], high birefringence [7], high numerical aperture [6], high nonlinear coefficient [8], large-mode-area [5] and endlessly sing-mode [4]. By using theoretical and experimental methods, the single-mode

[1] Erciyes University, Faculty of Science, Physics Department, Turkey, email: halimedemir@erciyes.edu.tr

behavior of PCFs is intensively studied [10, 11, 12, 13, 14, 15]. The dispersion calculations and measurements for PCFs with different structures are obtained [13, 14, 16, 17, 18, 19, 20, 21]. Until now, a plenty of variety methods has been used to work the characteristics properties of PCFs. The plane wave expansion method solving the full vectorial wave equation [22, 23, 24], as the name implies, is based on a plane wave expansion of the field and the position dependent dielectric constant in which equivalent to Fourier transform. It allows that the mode filed distribution and the photonic band gap of photonic crystal fiber and therefore the possible existence, width and positioning of photonic band gap can be calculated. The plane wave expansion of the periodic dielectric constant is simple and the coefficients of all terms are analytical but it will cost too much time; because it requires a large number of terms for expanding the field and the dielectric constant for certain accuracy [25]. Also, the plane wave expansion (PWE) method [26] requires a larger super cell. This larger super cell requires periodicity of the PCF cladding. The effective index (EI) method [27] is a scalar approach. In this method, PCF treats as an equivalance step index fiber. Thus, the birefringence and the mode field profile are can not obtain for PCFs. More effective methods than PWE are the supercell lattice method [30], the localized basis function method [28] and the multipole method [29]. However, these methods have restrictions in describing useful finite lattice periods, modal solutions near the cut-off region and the arbitral transverse change of the PCF cross-section, such as defining non-circular holes or non-identical multipole defects. Otherwise, in investigation of such complex structures the more powerful finite difference (FD) method [31], the finite element method (FEM) [32] and the beam propagation method (BPM) [33] are used. In this paper, the solid-core PCFs with triangular lattice was selected because of the simplicity of calculation and fabrication techniques. The single-mode behaviors and the mode-field areas of these PCFs are investigated for a fixed hole diameter (d) and a fixed pitch length (Λ), respectively by using PWE method. The applicability of the step-index fiber approximation to the this new type of fiber (PCF) has been examined.

2. PWE Method

In order to study the propagation of electromagnetic waves in PCFs it must solve Maxwell's equations with $\rho = 0$ and $\vec{J} = 0$. Taking the time dependence as given $\vec{H}(\vec{r},t) = \vec{H}(\vec{r})\exp(i\omega t)$, and because the PCF is a translationally invariant system along the longitudinal direction z of the PCF, one has $\vec{H}(\vec{r}) = \vec{H}(x,y)\exp(i\beta z)$, where β is the propagation constant. If we separate the fields into components transversal and parellel to the z axis:

$\vec{H}(\vec{r}) = (\vec{H}_t(x,y) + \hat{z}H_z(x,y))\exp(i\beta z)$ and from Maxwell's equations the transversal equations for the magnetic field $\vec{H}_t$ is obtained [26, 27]:

$$\left[\nabla_t^2 + \varepsilon(x,y)k_0^2 + \left(\frac{\nabla_t \varepsilon(x,y)}{\varepsilon(x,y)}\right)\times\nabla_t\times\right]\vec{H}_t(x,y) = \beta^2\vec{H}_t(x,y) \tag{1}$$

In order to obtain the guided modes of the structure, this equation must be solved subject to the boundary conditions (BCs). In a PCF, the core is surrounded by a medium, which can contain some hundreds of holes in a periodic pattern and solving Maxwell's equations applying the BCs in all the surfaces becomes an impossible task. However, a different approach is used to solve this equation. From Bloch's theorem, the eigenfunctions of the system can be written as

$$\vec{H}_t(\vec{r}) = \sum_G \vec{H}_t(\vec{G})\exp(i(\vec{k}+\vec{G}).\vec{r}) \tag{2}$$

where $\vec{r}, \vec{k}$ and $\vec{G}$ are two-dimensional vectors in the plane of periodicity. In Eq.1 the function $\varepsilon(x,y)$ and therefore $\ln\varepsilon(x,y)$, which comes from

$$\frac{\nabla_t \varepsilon(x,y)}{\varepsilon(x,y)} = \nabla_t\left[\ln(\varepsilon(x,y)\right] \tag{3}$$

are periodic functions in the x-y plane, so they can be expanded in a Fourier series. Once these expressions substitute in Eq.1 an eigenvalue equation for the propagation constant β is obtained. This method so-called plane-wave expansion (PWE) method is one of the methods widely used.

3. Single mode regime

Properties of standard fibers are frequently parameterized by the so-called *V*-parameter. The cut-off properties and endlessly single-mode phenomena of PCFs can be qualitatively understood by using it. The *V*-parameter for conventional step index optical fiber (SIF) is given by

$$V_{SIF} = \frac{2\pi}{\lambda} a\sqrt{n_{co}^2 - n_{cl}^2} \tag{4}$$

where λ is the operating wavelength, *a* is the core radius, n_{co} is the refractive index of core, n_{cl} is the refractive index of cladding. For the SIF the second order mode cut-off boundary is given by V_c = 2.405. For PCFs, having a cladding with a triangular lattice of air holes and a core formed by a missing air hole at the center of the structure, effective *V*-parameter is given by Mortensen at al.[12] as

$$V_{neff} = \frac{2\pi}{\lambda} \Lambda\sqrt{n_{eff}^2 - n_{FSM}^2} \tag{5}$$

where Λ is the pitch length of holes and n_{FSM} is the effective cladding index of the so-called fundamental space filling mode in the triangular air-hole lattice and $n_{eff}(\lambda) = c\beta/\omega$ is the "core index" associated with the effective index of the

fundamental mode. The cut-off condition of the second order mode for PCFs is given by $V^*_{n_{eff}} = \pi$. This means that the single-mode-regime of PCFs is characterized by $V_{n_{eff}} < V^*_{n_{eff}}$. Alternatively, Koshiba and Saitoh [14], according to the Eq.(4), defined *V*-parameter for PCFs:

$$V_{nco} = \frac{2\pi}{\lambda} a_{eff} \sqrt{n_{co}^2 - n_{FSM}^2} \tag{6}$$

where a_{eff} is the effective core radius that there was assumed to be $\Lambda/\sqrt{3}$. In this situation, the cut-off condition was given by $V^*_{n_{co}} = 2.405$, as in conventional SIFs. It is also numerically obtained that the single-mode-multimode boundary can be accounted for by the expression [34],

$$\frac{\lambda^*}{\lambda} \cong \alpha \left(\frac{d}{\Lambda} - \frac{d^*}{\Lambda} \right)^{\gamma} \tag{7}$$

where $\alpha = 2.80 \pm 0.12$, $\gamma = 0.89 \pm 0.02$ and $d^*/\Lambda = 0.406$ is the endlessly single-mode boundary. For $d/\Lambda > d^*/\Lambda$ the PCF supports a second order mode at wavelengths $\lambda/\Lambda < \lambda^*/\Lambda$ and is single mode for $\lambda/\Lambda > \lambda^*/\Lambda$.

4. Effective mode area

I have used the following Gaussian mode profile to obtain the effective mode-field-areas (MFA),

$$A_{eff} = \pi \omega_{eff}^2 \tag{8}$$

where ω_{eff} is the mode-field-radius (MFR). MFR is obtained by the Marcuse formula [35]:

$$\frac{\omega_{eff}}{a_{eff}} = 0.65 + \frac{1.618}{V_{eff}^{3/2}} + \frac{2.879}{V_{eff}^6} \tag{9}$$

5. Simulation Results

In this work, the PCFs are investigated with a core consist of a missing hole at the center in a silica background. Also, the PCFs studied in here have a cladding with a triangular lattice photonic crystal. This photonic crystal cladding is formed the air-holes with 4-rings around the core. The distance of the nearest two air-holes (pitch length) and the diameter of air-holes are given by *d* and Λ, respectively. For both fixed-*d* (*d* = 0.84 μm) and for the fixed-Λ (Λ = 4.2 μ*m*), I

have simulated the PCF structures for d/Λ interval from 0.1 to 0.7. For the wavelength of 1.55 μm, the core index is taken to be 1.45.

Here, to calculate the effective index of the fundamental modes of the solid-core PCFs, I have used the BandSolve [36] software based on plane wave expansion (PWE) method [26]. The core material refractive indices are obtained from Selmeier's formula of the material [37].

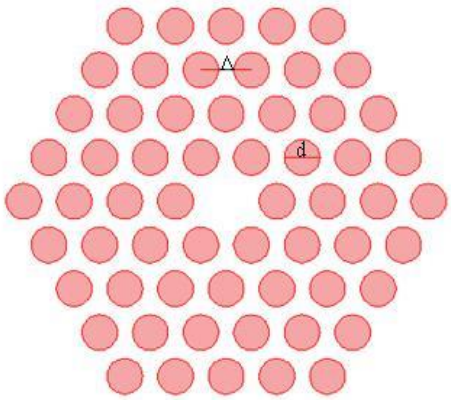

Fig. 1. The cross-section of the solid core PCF

In calculations, $V_{n_{co}}$ is taken as V_{eff} in Eq.(9). The effective V-parameters versus wavelength for different d/Λ ratios are calculated from Eqs.(5), (6) and plotted in Fig.2 for the structures of fixed-d and of fixed-Λ, respectively. As seen from the figures, there is no significant difference to conclude if PCF is in the single mode region by using $V^*_{n_{eff}} = \pi$ or $V^*_{n_{co}} = 2.405$ from the corresponding curves. The fixed-d structures are working under the single-mode regime for the d/Λ values smaller than 0.7 within the wavelength range from 0.8 to 2.0 μm, but for the fixed-Λ structures, the boundary for the single-mode regime is $d/\Lambda < 0.5$. In order to compare the single-mode behaviors of the structures examined, for the wavelength of 1.55 μm, V_{eff} , n_{eff} and n_{FSM} versus d/Λ are plotted in Fig.3 for the fixed-d and for the fixed-Λ respectively. It is clear from Fig.3 that the fixed-d structures are working under the single-mode regime for all the d/Λ values considered, but for the fixed-Λ structures there is boundary for d/Λ about 0.55 for working in single-mode regime.

Also, in comparison with the structures with fixed-Λ, the V-parameter and thus the number of guided modes is higher for fixed-d. This difference between V -parameters of the structures with fixed-Λ and fixed-d is due to the behavior of the refractive index of the fundamental space filling mode n_{FSM} . As

can be seen from Fig.6, for the fixed-*d* and fixed-Λ, the difference between the n_{FSM} values increase as the d/Λ ratios increase. The n_{FSM} values of the structures with fixed-*d* are generally smaller than those of the structures with fixed-Λ. For fixed-*d*, the *V*-parameter values decrease with wavelength more rapidly than those of the structures with fixed-Λ, in particular for the d/Λ values larger than 0.5. The reason for this situation, for the fixed-*d*, the *V*-parameter in Eq.(4) is depend on both n_{FSM} and a_{eff} , which are also depend on wavelength. However, the *V*-parameter is only depend on n_{FSM} for the fixed-Λ.

A similar study of effective *V*-parameter of PCFs has been done in Ref. [38], in which the core formed by one missing hole at the center of the photonic crystal structure with square lattice of four rings of air holes. The refractive index of the silica background and solid core is n_{co} = 1.45. The effective *V*-parameter values and single-mode regime have been obtained for the PCFs with the circular and square air holes.

The obtained values of the single-mode regime for the PCFs have been compared in Table1 with that of the [38]. As can be seen in Table1, there is no significant difference between the single-mode regime of both structures. The type of lattice has no significant effect on the number of guided modes and the single mode region.

The refractive index differences ($\Delta n = n_{eff} - n_{FSM}$) of the structures, which determines the confinement and the leakage and hence mode-field-radius, versus the wavelength are plotted in Fig.4. The refractive index differences remain almost constant with wavelength for $d/\Lambda \leq 0.3$ and have the similar values for the both structures, but for the fixed-*d* structures their values are greater than those for the fixed-Λ structures for the values of $d/\Lambda \leq 0.5$ and have a small oscillation with wavelength about some average value (Fig.4a) while they changes almost linearly with wavelength for the fixed-Λ structures (Fig.4b). The effective-mode-areas at the wavelength of 1.55 μ*m* of the struc-tures are plotted in Fig.5. A_{eff} values for the fixed-Λ are larger than those of the fixed-*d* structures (Fig.5b); additionally for d/Λ values smaller than 0.2, it increases more rapidly than that of the fixed-*d* structures with decreasing d/Λ (Fig.5a). This behaviour can be clarified by addressing to Fig.2, Fig.3 and Fig.4. For the fixed-Λ, the effective mode-field-radius ω_{eff} , which is concerned with A_{eff} via Eq.8, has a reciprocal proportionality with only V_{eff} due to the effective core radius is taken as a constant ($a_{eff} = \Lambda/\sqrt{3}$). On the contrary, for the fixed-*d*, $A_{ef\,f}$ is related to both $V_{ef\,f}$ and $a_{ef\,f}$ which are change with They are equal to each other for the two structures at the $d/\Lambda = 0.2$, for which the two structures become identical.

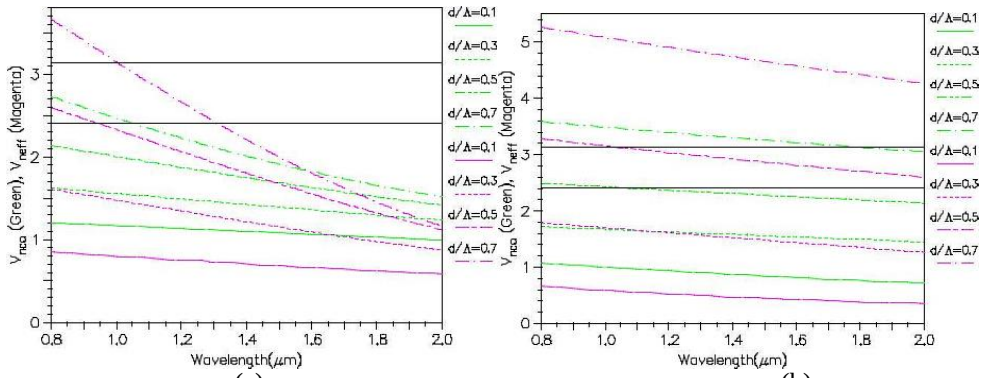

(a) (b)

Fig. 2. The *V*-parameter as a function of the wavelength for a) the fixed-*d*, b) the fixed-Λ

Finally, I obtained the fields and energy distributions of the structures. For the fixed-d and fixed-Λ, the PCFs with d/Λ=0.1 and 0.3 are in the single-mode regime for both Eq.5 and Eq.6. The light is well confined in the core region for d/Λ=0.3. Therefore, the fields and energy distributions of the structure for d/Λ = 0.3 are given in the Fig.6 and Fig.7, respectively.

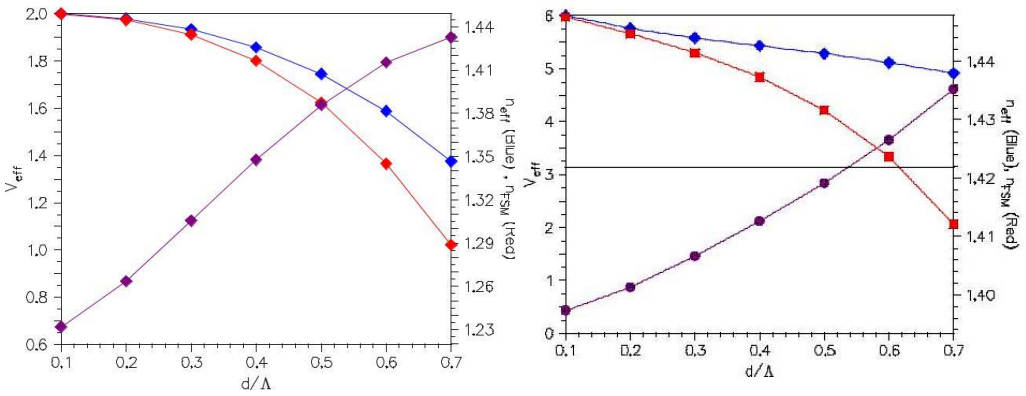

(a) (b)

Fig. 3. The V_{neff} parameter, n_{eff} and n_{FSM} variation with d/Λ for a) the fixed-*d* b) for the fixed Λ at 1.55 μ*m*

Table 1.

The single-mode regime for PCFs with the hexagonal and square lattice

Type of lattice		Fixed Λ = 4.2 μ*m*		Fixed *d* = 0.84 μ*m*
	d/Λ	Single-mode regime (μ*m*)	*d*/Λ	Single-mode regime (μ*m*)
	0.1	0.8-2.0	0.1	0.8-2.0
Hexagonal	0.3	0.8-2.0	0.3	0.8-2.0
	0.5	1.0-2.0	0.5	0.8-2.0

	0.7	-	0.5	1.05-2.0
	0.1	0.8-2.0	0.1	0.8-2.0
Square [38]	0.3	0.8-2.0	0.3	0.8-2.0
	0.5	1.05-2.0	0.5	0.8-2.0
	0.7	-	0.7	1.15-2.0

For the fixed-Λ, the electric and magnetic field distributions are more extended into the cladding region (i.e. guiding is weakened). The effective index of the fundamental mode becomes complex and thus the mode becomes leaky. As a result of this, the energy intensity transported in the core region is also reduced. The reason of this behavior is that the effective cladding index approaches the core index and hence the index difference decreases.

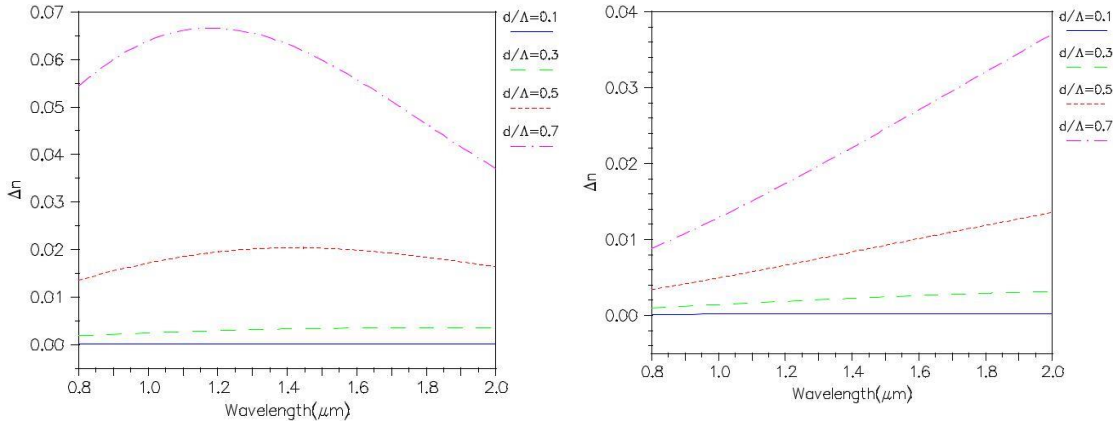

Fig. 4. The refractive index differences ($\Delta n = n_{eff} - n_{FSM}$) versus the wavelength (a) for the fixed-*d* structures, (b) for the fixed-Λ structures.

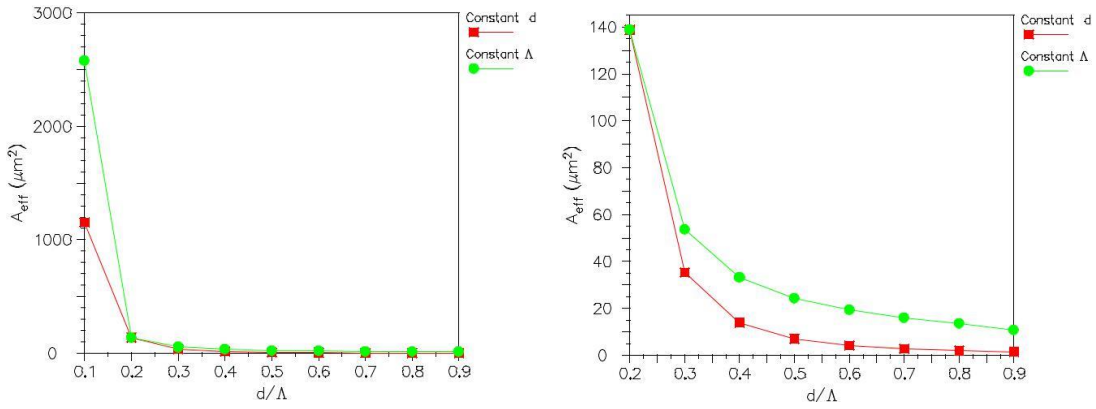

(*a*) (b)

Fig. 5. The effective-mode-area of the structures considered for Λ = 1.55 μ*m* of the structures considered (a) *d*/Λ = 0.1−0.9, (b) *d*/Λ = 0.2−0.9.

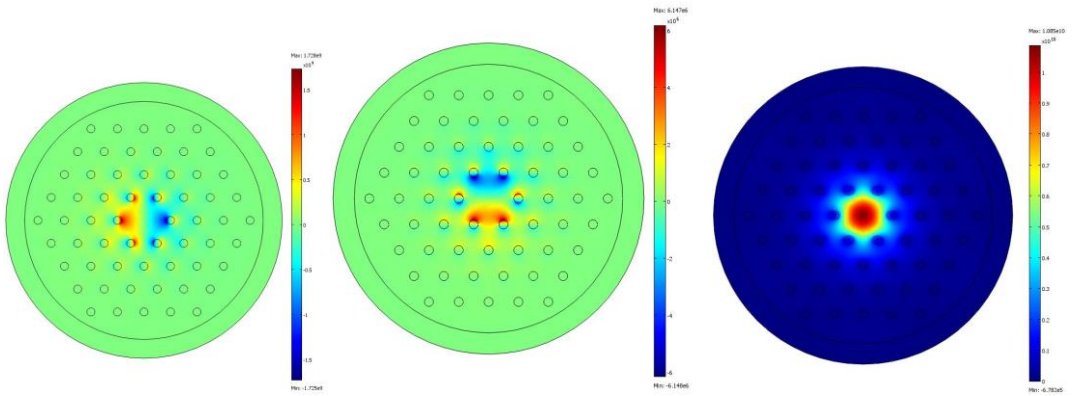

(a) (b) (c)

Fig. 6. For fixed-d and λ=1.55 μm (a) the distribution of *z*- component of the electric field, (b) the distribution of *z*- component of the magnetic field, (c) the total energy ddistribution.

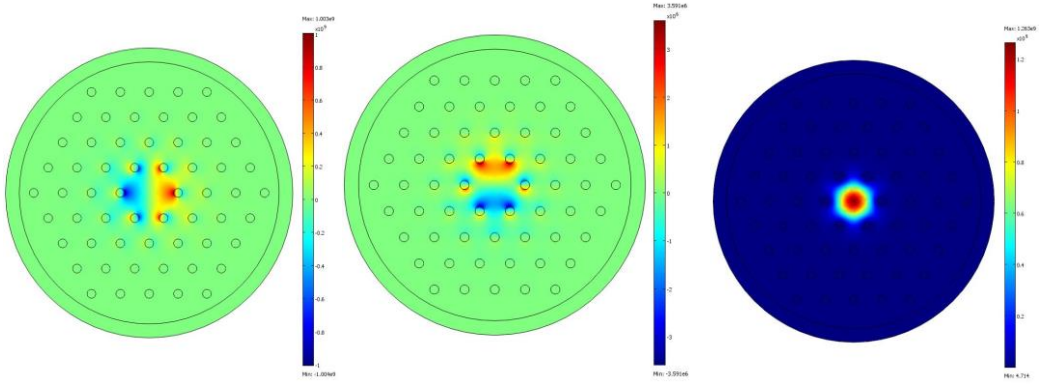

(a) (b) (c)

Fig. 7. For fixed-Λ and λ=1.55 μm (a) the distribution of *z*- component of the electric field, ((b) the distribution of *z*- component of the magnetic field, (c) the total energy ddistribution.

6. Conclusion

It is concluded from the simulations that, in order to conclude the PCF is in the single-mode regime or not, there is no significant difference between using the direct evaluation of the *V*-parameter of photonic crystal fiber and step-index fiber analogy, but using the SIF approximation is a more straightforward method, especially for estimation of effective-mode-area. For the fixed-*d*, V_{eff} decreases with wavelength and reaches the single-mode limit more rapidly than those of fixed-Λ structures for especially $d/\Lambda > d^*/\Lambda$. For an operation wavelength of 1.55 μm, which is widely used in fiber optics and photonics, the fixed-*d* structures studied are all in the single mode regime for the range of d/Λ considered.

Effective mode area of PCFs considered is larger for the fixed-Λ than those of the fixed-*d* structures for every d/Λ ratio and reaches some values larger than 1000 μm^2 for the d/Λ values smaller than 0.2. It is worth to pay attention that, great level of flexibility in the PCF manufacturing, processes and methods for postprocessing gives us a high flexibility to arrange the design parameters of PCFs having the requested properties.

REFERENCES

[1] *J. C. Knight, T. A. Birks, P. St. J. Russell and D. M. Atkin*, All-silica single-mode optical fiber with photonic crystal cladding, Opt. Lett., **21** (1996), 1547-1549.

[2] *J. C. Knight, J. Broeng, T. A. Birks and P. St. J. Russell*, Photonic Band Gap Guidance in Optical Fibers, Science, **282** (1998), 1476-1478.

[3] *T. A. Birks, J. C. Knight and P. St. J. Russell*, Endlessly single-mode photonic crystal fiber, Opt. Lett., **22** (1997), 961-963.

[4] *L. Xiao, W. Jin and M. S. Demokan*, Photonic crystal fibers confining light by both index-guiding and bandgap-guiding: hybrid PCFs, Opt. Exp., **15** (2007), 15637-15647.

[5] *J. C. Knight, T. A. Birks, R. F. Cregan, P. St. J. Russell and P. D. De Sandro*, Large mode area photonic crystal fibre, Electron. Lett., **34** (1998), 1347-1348.

[6] *W. J. Wadsworth, R. Percival, G. Bouwmans, J. C. Knight and P. St. J. Russell*, High power air-clad photonic crystal fibre laser, Opt. Exp., **11** (2003), 48-53.

[7] *A. Ortigosa-Blanch, J. C. Knight, W. J. Wadsworth, J. Arriaga, B. J. Mangan, T. A. Birks and P. St. J. Russell*, Highly birefringent photonic crystal fibers, Opt. Lett., **25** (2000), 1325-1327.

[8] *P. Petropoulos, T. M. Monro, W. Belardi, K. Furusawa, J. H. Lee and D. J. Richard-son*, 2R-regenerative alloptical switch based on a highly nonlinear holey fiber, Opt. Lett., **26** (2001), 1233-1235.

[9] *T. A. Birks, D. Mogilevstev, J. C. Knight and P. St. J. Russell*, Dispersion compensation using single material fibers, IEEE Photon. Technol. Lett., **11** (1999), 674-676.

[10] *N. Kejalakshmy, B. M. A. Rahman, A. K. M. S. Kabir, M. Rajarajan and K. T. V. Grattan*, Single mode operation of photonic crystal fiber using a full vectorial finite element method, Proc. of SPIE, **6588** (2007), 65880T.

[11] *Z. Chen, J. Hou, X. Xi, G. Sun and Z. Jiang*, Endlessly single-mode operation of highly nonlinear photonic crystal fibers by controlled hole collapse, Opt. Commun., **283** (2010) 4645-4648.

[12] *N. A. Mortensen, M. D. Nielson, J. R. Folkenberg, A. Petersson and H. R. Simonsen*, Improved large-mode-area endlessly single-mode photonic crystal fibers, Opt. Lett., **28** (2003), 393-395.

[13] *J. Broeng, D. Magilevstev, S. E. Barkou and A. Bjarklev*, Photonic Crystal Fibers: A New Class of Optical Waveguides, Opt. Fiber Technol., **5** (1999), 305-330.

[14] *M. Koshiba and K. Saitoh*, Applicability of classical optical fiber theories to holey fibers, Opt. Lett., **29** (2004), 1739-1741.

[15] *N. A. Mortensen, J. R. Folkenberg, M. D. Nielson and K. P. Hansen*, Modal cut-off and the V-parameter in photonic crystal fibers, Opt. Lett., **28** (2003), 1879-1881.

[16] *M. Chen and S. Xie*, New nonlinear and dispersion flattened photonic crystal fiber with low confinement loss, Opt. Commun., **281** (2008), 2073-2076.

[17] *K. M. Gundu, M. Kolesik, J. V. Moloney and K. S. Lee*, Ultra-flattened dispersion selectively liquid-filled photonic crystal fibers, Opt. Express, **14** (2006), 6870-6878.

[18] *W. H. Reeves, J. C. Knight, P. St. J. Russell and P. J. Roberts*, Demonstration of ultra-flattened dispersion in photonic crystal fibers, Opt. Express, **10** (2002), 609-613.

[19] *K. M. Ferrando, E. Silvestre, P. Andres, J. J. Miret and M. V. Andres*, Designing the properties of dispersion-flattened photonic crystal fibers, Opt. Express, **9** (2001), 687-697.

[20] *L. P. Shen, W. P. Huang and S. S. Jian*, Design of photonic crystal fibers for dispersion-related applications, J. Lightwave Technol., **21** (2003), 1644-1651.

[21] *Y. L. Hoo, W. Jin, J. Ju, H. L. Ho and D. N. Wang*, Design of photonic crystal fibers with ultra-low, ultra-flattened chromatic dispersion, Opt. Commun., **242** (2004), 327-332.

[22] *S. E. Barkou, J. Broeng and A.Bjarklev*, Dispersion properties of photonic bandgap guiding fibers, in Optical Fiber Communication Conference, OSA, Washington D. C., FG5, (1998), 117-119.

[23] *J. D. Joannopoulos, R. D. Meade and J. N. Winn*, Photonic crystals: molding the flow of light, Princeton U. Pres, New York, (1995).

[24] *W. H. Reeves, J. C. Knight, P. St. J. Russell and P. J. Roberts*, Demonstration of ultra-flattened dispersion in photonic crystal fibers, Opt. Express, **10** (2002), 609-613.

[25] *K. M. Ferrando, E. Silvestre, P. Andres, J. J. Miret and M. V. Andres*, Designing the properties of dispersion-flattened photonic crystal fibers, Opt. Express, **9** (2001), 687-697.

[26] *L. P. Shen, W. P. Huang and S. S. Jian*, Design of photonic crystal fibers for dispersion-related applications, J. Lightwave Technol., **21** (2003), 1644-1651.

[27] *Y. L. Hoo, W. Jin, J. Ju, H. L. Ho and D. N. Wang*, Design of photonic crystal fibers with ultra-low, ultra-flattened chromatic dispersion, Opt. Commun., **242** (2004), 327-332.

[28] *S. E. Barkou, J. Broeng and A.Bjarklev*, Dispersion properties of photonic bandgap guiding fibers, in Optical Fiber Communication Conference, OSA, Washington D. C., FG5, (1998), 117-119.

[29] *J. D. Joannopoulos, R. D. Meade and J. N. Winn*, Photonic crystals: molding the flow of light, Princeton U. Pres, New York, (1995).

[30] *S. Guo and S. Ablin*, Simple plane wave implementation for photonic crystal calculations, Opt. Express., **11** (2003), 167-175.

[31] *W. Zhi, et al.*, Supercell lattice method for photonic crystal fibers, Optics Express., **11** (2003), 980-991.

[32] *J. Arriaga, J. C. Knight and P. St. J. Russell*, Modeling the propagation of light in photonic crystal fibers, Physica D-Nonlinear Phenomena, **189** (2004), 100-106.

[33] *J. C. Knight, T. A. Birks, P. St. J. Russell and J. P. De Sandra*, Properties of photonic crystal fiber and the effective index model, J. Opt. Soc. Am. A, **15** (1998), 748-752.

[34] *T. M. Monro, D. J. Richardson, N. G. R. Broderick and P. J. Bennet*, Holey optical fibers: an efficient modal model, J. Lightwave Technol., **17** (1999), 1093-1102.

[35] *T. P. White, R. C. McPhedran, C. M. De Sterke, L. C. Botten and M. J. Steel*, Confinement losses in microstructured optical fibers, Opt. Lett., **26** (2001), 1660-1662.

[36] *Z. Wang, R. Guobin, L. Shuqin and J. Shuisheng*, Supercell lattice method for photonic crystal fibers, Opt. Express, **11** (2003), 980-991.

[37] *J. Riishede, N. A. Mortensen and J. Laegsgaard*, A 'poor man's approach' to modelling micro-structured optical fibres, J. Optics A-Pure and Appl. Optics, **5** (2003), 534-538.

[38] *B. M. A. Rahman, A. K. M. S. Kabir, M. Rajarajan and K. T. V. Grattan*, Finite element modal solutions of planar photonic crystal fibers with rectangular air-holes, Opt. and Quantum Electron., **37** (2005), 171-183.

[33] *F. Fogli, L. Saccomandi, P. Bassi, G. Bellanca and S. Trillo*, Full vectorial BPM modelling of index guiding photonic crystal fibers and couplers, Opt. Express, **10** (2002), 54-59.

[34] *B. T. Kulhmey, R. C. McPhedran and C. M. Sterke*, Modal cutoff in microstruc- tured optical fibres, Opt. Lett., **27** (2002), 1684-1686.

[35] *D. Marcuse*, Loss analysis of single-mode fiber splices, Bell Syst. Tech. J. **56** (1977), 703-718.

[36] RSoft Design Group, www.rsoftdesign.com

[37] *A. Bjarklev, J. Broeng and A. S. Bjarklev*, Photonic Crsytal Fibres, Kluwer Academic Publishers, Dordreeht, 2003.

[38] *H. Demir and S. Ozsoy*, Solid-core square-lattice photonic crystal fibers: comparative studies of the single-mode regime and numerical aperture for circular and square air-holes, Opt. Quant. Electron., **42** (2011), 851-862.